Journal of Pathology
J Pathol 2002; **198**: 142–156.
Published online 18 April 2002 in Wiley InterScience (www.interscience.wiley.com). **DOI:** 10.1002/path.1121

Original Paper

Transcription factor E2F-1 acts as a growth-promoting factor and is associated with adverse prognosis in non-small cell lung carcinomas

Vassilis G Gorgoulis,[1]* Panayotis Zacharatos,[1] George Mariatos,[1] Athanassios Kotsinas,[1] Martha Bouda,[1] Dimitris Kletsas,[2] Panayiotis J Asimacopoulos,[3,4] Niki Agnantis,[5] Christos Kittas[1] and Athanasios G Papavassiliou[6]

[1] *Molecular Carcinogenesis Group, Department of Histology and Embryology, School of Medicine, University of Athens, Greece*
[2] *Laboratory of Cell Proliferation and Ageing, Institute of Biology, NCSR Demokritos, Athens, Greece*
[3] *Department of Cardiac Surgery, School of Medicine, University of Athens, Greece*
[4] *Baylor College of Medicine, Houston, Texas, USA*
[5] *Department of Pathology, School of Medicine, University of Ioannina, Ioannina, Greece*
[6] *Department of Biochemistry, School of Medicine, University of Patras, Patras, Greece*

**Correspondence to:*
Dr Vassilis G Gorgoulis,
Antaiou 53 Str, Lamprini, Ano Patissia, GR-11146 Athens, Greece.
E-mail: histoclub@ath.forthnet.gr

Received: 18 June 2001
Revised: 9 October 2001
Accepted: 4 February 2002

Abstract

Numerous upstream stimulatory and inhibitory signals converge to the pRb/E2F pathway, which governs cell-cycle progression, but the information concerning alterations of E2F-1 in primary malignancies is very limited. Several *in vitro* studies report that E2F-1 can act either as an oncoprotein or as a tumour suppressor protein. In view of this dichotomy in its functions and its critical role in cell cycle control, this study examined the following four aspects of E2F-1 in a panel of 87 non-small cell lung carcinomas (NSCLCs), previously analysed for defects in the pRb-p53-MDM2 network: firstly, the status of E2F-1 at the protein, mRNA and DNA levels; secondly, its relationship with the kinetic parameters and genomic instability of the tumours; thirdly, its association with the status of its transcriptional co-activator CBP, downstream target PCNA and main cell cycle regulatory and E2F-1-interacting molecules pRb, p53 and MDM2; and fourthly, its impact on clinical outcome. The protein levels of E2F-1 and its co-activator CBP were significantly higher in the tumour area than in the corresponding normal epithelium ($p < 0.001$). E2F-1 overexpression was associated with increased *E2F-1* mRNA levels in 82% of the cases examined. The latter finding, along with the low frequency of *E2F-1* gene amplification observed (9%), suggests that the main mechanism of E2F-1 protein overexpression in NSCLCs is deregulation at the transcriptional level. Mutational analysis revealed only one sample with a somatic mutation at codon 371 (*Glu* → *Asp*) and one carrying a polymorphism at codon 393 (*Gly* → *Ser*). Carcinomas with increased E2F-1 positivity demonstrated a significant increase in their growth indexes ($r = 0.402$, $p = 0.001$) and were associated with adverse prognosis ($p = 0.033$ by Cox regression analysis). The main determinant of the positive association with growth was the parallel increase between E2F-1 staining and proliferation ($r = 0.746$, $p < 0.001$), whereas apoptosis was not influenced by the status of E2F-1. Moreover, correlation with the status of the pRb-p53-MDM2 network showed that the cases with aberrant pRb expression displayed significantly higher E2F-1 indexes ($p = 0.033$), while a similar association was noticed in the group of carcinomas with deregulation of the p53-MDM2 feedback loop. In conclusion, the results suggest that E2F-1 overexpression may contribute to the development of NSCLCs by promoting proliferation and provide evidence that this role is further enhanced in a genetic background with deregulated pRb-p53-MDM2 circuitry. Copyright © 2002 John Wiley & Sons, Ltd.

Keywords: E2F-1; CBP; pRb; p53; MDM2; proliferation; apoptosis; prognosis; lung cancer

Introduction

The cell cycle clock apparatus acts as a master controller supervising the decision of the cell to proliferate, to enter into reversible quiescence, to differentiate, or to die by activating the apoptotic process. Deregulation of the cell cycle process represents an imperative step for malignant transformation. The E2F family of transcription factors plays a pivotal role in cell cycle control and apoptosis, while recent studies suggest that they are also involved in the regulation of developmental control genes. In mammals, the E2F family has six identified members (E2F-1 to E2F-6), in three groups based on differing homology. The best-characterized member of the family is E2F-1 [1,2].

The *E2F-1* gene is mapped at chromosomal region 20q11 and encodes a 437-amino acid (aa), 60 kDa nuclear DNA-binding protein, originally identified through its role in transcriptional activation of the adenovirus E2 promoter [3]. Structural analysis of E2F-1 has identified five functional domains ([2,3] and references therein). At the N-terminus, E2F-1 has a cyclin A-binding site (aa positions 67–108), followed by the DNA-binding (aa positions 128–181), dimerization (aa positions 199–239) and 'marked-box' domains (aa positions 244–309). At the C-terminal region lies the transactivation domain (aa positions 369–437), which is responsible for binding to the 'pocket' protein family of tumour suppressors (pRb (aa positions 407–426), p107 and p130). The E2F-binding activity peaks at the G1-S phase boundary and comprises a heterodimer of E2F and a member of the DP family [4–7]. The ability of the E2F-1/DP complex to stimulate transcription is mainly dependent on the phosphorylation state of pRb [1,2]. Active (hypophosphorylated) pRb 'masks' and inactivates the activation domain of E2F-1 by competing with factors which positively affect transcription, such as TBP [8], TFIIH [9], MDM2 (aa positions 380–407) [10] and CBP/p300 (aa positions 426–437) [11]. In addition, recent reports demonstrate that pRb, apart from its 'masking' effect on E2F-1, has the capacity to repress potently E2F-1 targets by recruiting histone deacetylase 1 (HDAC1), which suppresses transcription by modifying histones or other promoter-bound transcription factors [12,13]. On the other hand, hyperphosphorylation (inactivation) of pRb by cyclin-cdk complexes releases E2F-1, which induces expression of E2F-1 target genes. These genes bear the E2F recognition sequence [TTT (G/C) (G/C) CG (G/C)] [6] and are implicated in: (i) DNA synthesis (e.g. dihydrofolate reductase (DHFR), thymidine kinase (TK), DNA polymerase-α, PCNA, CDC6, ORC1), (ii) cell-cycle control (e.g. cyclin E, cyclin A, cdk2 and 4, cdc2), (iii) 'pocket' protein expression (pRb, p107), (iv) proto-oncogene regulation (e.g. myb, myc), (v) E2F-1 and E2F-2 transcription [1,2,7,14] and (vi) p53 stabilization by inducing the expression of $p14^{ARF}$ [15]. Regarding the latter, indirect relationship between E2F-1 and p53, current studies demonstrate that E2F-1 can directly bind to p53, an interaction which appears to downregulate the activity of both factors [16].

The role of E2F-1 is currently under intensive investigation in view of its *dual* cellular behaviour in *cell lines and transgenic models* and thus it is a matter of debate among various study groups. On one hand, evidence has shown that transcriptional activation by E2F-1 is important in promoting cell proliferation [2,7,17–19]. Moreover, the ability of E2F-1 to transform cells in classical oncogene cooperation experiments and to produce tumours in nude mice supports its putative role as an oncogene [20,21]. On the other hand, $E2F-1^{-/-}$ knockout mice suffer a significant increase in the incidence of tumours, implying that E2F-1 is also endowed with growth inhibitory and tumour suppressor activities [22–28]. Most of this information comes from *in vitro* studies, which makes it hard to draw definite conclusions about the role of E2F-1 *in vivo*. Although the data concerning E2F-1 status in tumours are very limited [29–34], it seems that a dual role exists here as well. Rabbani *et al*. suggested a tumour suppressor role for E2F-1 in bladder cancer [31], whereas Zhang *et al*. observed a positive correlation between E2F-1 and proliferation index in breast neoplasia [29]. These findings imply a tissue-specific effect and it is therefore necessary to obtain information concerning its status and possible role in primary malignancies.

In view of its critical and controversial role in cell cycle control, we examined the following aspects of E2F-1 in a panel of 87 NSCLCs, previously analysed for defects in the pRb-p53-MDM2 network [35,36]: (i) the status of E2F-1 at the protein, mRNA, and DNA levels; (ii) its relationship with the kinetic parameters (proliferation and apoptosis) and genomic instability of the tumours; (iii) the status of its transcriptional co-activator CBP; (iv) its association with the main cell cycle regulatory and E2F-1-interacting molecules, pRb, p53 and MDM2 and downstream target PCNA; and finally, (v) its impact on patient outcome.

Materials and methods

Tissue samples

Frozen and formalin-fixed paraffin-embedded (FFPE) material from a total of 87 surgically removed NSCLCs and adjacent normal lung tissue were analysed. These tumours were classified according to the WHO criteria and the TNM system, and had previously been investigated for the G1 phase protein network pRb-p53-MDM2 [35,36]. Two samples of each tumour were taken, one snap-frozen in liquid nitrogen and stored at $-70\,^{\circ}C$, the other formalin-fixed and paraffin-embedded. In addition, adjacent normal tissue was included from each specimen examined. The patients had not undergone any chemo- or radiotherapy prior to surgical resection, thus avoiding upregulation of p53 and pRb and down-regulation of MDM2, due to DNA damage ([35,36] and references therein). Clinicopathological features of the patients are presented in Table 1.

Immunohistochemistry

Antibodies

For immunohistochemical analysis the following antibodies (Abs) were used: KH95 (Class: IgG2a mouse monoclonal; epitope: Rb-binding domain of E2F-1 p60, human origin) (Santa Cruz, Bioanalytica, Greece) and anti-CBP (C-1) (Class: IgG1 mouse monoclonal;

Table 1. Summary of E2F1, pRb, p53 and MDM2 status, kinetic parameters, ploidy and clinicopathological features

E2F1 status (normal-tumour tissue comparison)			
Immunohistochemical evaluation (IHC)[a]	M (n): 45.7% (79)	SD: 14.9%	
mRNA levels	elevated (n): 82% (79)		
gene status	amplification (n): 9% (79)		
mutation analysis[b]	mutation (n): 2 (79)		
Proliferation index (%)[c]	M (n): 35.2% (80)	SD: 11.3%	
Apoptotic index (%)[d]	M (n): 2.04% (72)	SD: 2.06%	
Growth index (%)	M (n): 39.6% (70)	SD: 43.2%	
Ploidy status	A: 46	D: 34	
CBP status[e]	M (n): 65.3% (76)	SD: 7.7%	
pRB status[f]	Ab: 34	No: 52	
p53 status[f]	P: 49	N: 37	
MDM2 status[f]	P: 57	N: 29	
Histology	ADCs: 41	SCCs: 41	UL: 5
Lymph node invasion	yes: 47	No: 39	
Tumour stage	I: 35	II: 28	III: 23
Survival status[g]	deceased (MD): 44 (14)	alive (MD): 41 (34)	

Abbreviations: M, mean value; SD, standard deviation; n, number of informative samples; Ab, aberrant; No, normal; P, positive; N, negative; ADC, adenocarcinoma; SCC, squamous cell carcinoma; UL, undifferentiated large cell carcinoma; MD, median value (in months after surgery).

[a] Normal tissue E2F1 IHC status: $12.1 \pm 2.3\%$.

[b] Mutation analysis of the DNA-binding (exon 3) and transactivation (exon 7) domains, Gly393Ser polymorphism (case 19) and tumour-specific mutation Glu371Asp (case 47).

[c] Estimated by MIB-1 immunohistochemistry.

[d] Estimated by TUNEL assay.

[e] Normal tissue CBP IHC status: $15.4 \pm 3.1\%$.

[f] Data from our previous studies [35,36]: p53 and MDM2 positivity was significantly associated with p53 mutations and MDM2 mRNA increased levels, respectively.

[g] Follow-up up to 5 years.

epitope: carboxy terminus of CBP of human origin) (Santa Cruz, Bioanalytica, Greece).

Method

Immunohistochemistry was performed according to the indirect streptavidin–biotin–peroxidase method, as previously described [35,36] with a modification in the heat-mediated antigen retrieval method. In brief, 5 μm paraffin sections were mounted on poly-L-lysine-coated slides, dewaxed, rehydrated and incubated for 30 min with 0.3% hydrogen peroxide to quench the endogenous peroxidase activity. Unmasking of the related proteins was carried out in a 1 mM EDTA pH 8 solution for half an hour in a steamer (Temperature around 95 °C). The sections were incubated with the primary antibody at a 1 : 100 dilution at 4 °C overnight. Biotin-conjugated secondary antibody was added at a 1 : 200 dilution for 1 h at room temperature (RT). The next stage comprised 30 min incubation in StreptAB Complex (1 : 100 stock biotin solution, 1 : 100 stock streptavidin-peroxidase solution) (Dako, Kalifronas, Greece). For colour development we used 3, 3′-diaminobenzidine tetrahydrochloride (DAB) and haematoxylin as counterstain.

Evaluation

Only nuclear staining was considered positive. An average of 500 cells were counted at ×400 in each case. The E2F-1 and CBP status was assessed as the percentage of stained tumour nuclei. Three independent observers (V.G., P.Z. and C.K.) carried out slide examination. Inter-observer variability was minimal ($p < 0.01$).

Controls

The MCF-7 cell line (derived from breast cancer) was used as positive control for E2F-1 expression [29]. The specificity of anti-CBP antibody was tested by incubating the latter with the appropriate control peptide (Santa Cruz, Bioanalytica, Athens, Greece), against which it was raised. Elimination of immunostaining verified CBP positivity. In each set of immunoreactions, antibody of the corresponding IgG fraction, but of unrelated specificity was used as a negative control.

Protein extraction and western blot analysis

Protein extraction

Frozen fresh tissue samples were homogenized in 50 mM Hepes pH 7.5, 150 mM NaCl, 15 mM β-mercaptoethanol, 0.5 mM PMSF, 0.1% NP40 (Sigma, Athens, Greece). The homogenate was centrifuged at 3000 rpm ($1000 \times g$) at 4 °C for 5 min. The supernatant was collected and adjusted to 1 μg/ml aprotinin, 1 μg/ml leupeptin and 1 μg/ml pepstatin A (Merck, Athens, Greece).

Antibodies and controls

The anti-E2F-1 KH95 and anti-CBP (C-1) mouse monoclonal antibodies (Santa Cruz Biotechnology, Bioanalytica, Athens, Greece) were used as first antibodies, while a goat anti-mouse IgG (H + L) horseradish peroxidase-labelled secondary antibody was employed (31430, Pierce, Bioanalytica, Athens, Greece). The human tumour cell line MCF-7, known to overexpress E2F-1 [29] and the HeLa cell line, which expresses CBP, were used as positive controls. The anti-actin C-2 mouse monoclonal antibody (Santa Cruz Biotechnology, Bioanalytica, Athens, Greece) was used for assessing equal loading of total protein per sample.

Gel electrophoresis and blotting

10 μg total protein from each sample were adjusted with SDS PAGE sample buffer (NEB, Bioline, Athens, Greece) and loaded on 4–20% gradient PAGEr™ Gold precast gels (Biowhittaker, Bioanalytica, Athens, Greece). Gel electrophoresis and transfer to nitrocellulose membranes (Protran BA85, Schleicher & Schuell) were performed according to standard protocols [37].

Signal development and quantitation

Blots were blocked for 1 h in 5% non-fat dry milk/TBS-T (TBS-T: TBS, 0.1% Tween-20) at RT. Subsequently, membranes were incubated overnight with primary antibody (sc-251, 1/500 dilution) at 4 °C, followed by 1 h incubation with secondary peroxidase-labelled antibody (1/50 000 dilution) at RT. Signal development for E2F-1 was performed with the enhanced SuperSignal West Pico Chemiluminescent Substrate (Pierce, Bioanalytica, Athens, Greece). Actin detection was performed in a similar manner. Autoradiographs were scanned on a flatbed scanner and band intensities were estimated with Image-Pro Plus software, Version 3.0 for Windows (Media Cybernetics, Silver Spring, USA).

Microdissection and nucleic acid extraction

Microdissection

For DNA extraction, contiguous 5 μm sections were processed. The first section was stained with haematoxylin and eosin to visualize the extent of tumour cells within each sample. The boundaries of the cancerous tissue were delineated microscopically and excess normal tissues were removed using sterile surgical blades, as previously described [35,36].

DNA extraction

DNA extraction was performed using the phenol-chloroform-isoamyl alcohol procedure following tissue digestion with proteinase K [37].

RNA extraction-cDNA synthesis

Material with excess tumour tissue was used for RNA extraction, because microdissection is not suitable for RNA-handling methods. RNA was extracted with Trizol reagent (Life Technologies, AntiSel, Greece), according to the manufacturer's instructions. cDNA was generated using M-MLV reverse transcriptase (Life Technologies, AntiSel, Greece) and oligo-dT_{18} (Life Technologies, AntiSel, Greece), as previously described [35].

Comparative reverse transcription (RT)-PCR

E2F-1 and *PCNA* mRNA levels were assessed with a semi-quantitative multiplex RT-PCR method, as described previously [36,38]. Target *E2F-1* or *PCNA* cDNA fragment was co-amplified with a larger reference cDNA fragment of *β-actin* or *GAPDH*, respectively. The relative ratios of the amplified products in the tumour samples reflect the relative proportion of input mRNAs and were compared with the relative ratios of the corresponding normal tissue.

Primers

The primers used for targeting *E2F-1* and *PCNA* are presented in Table 2.

Table 2. Amplimers and thermal profiles for each segment

Segment	Amplimers				Thermal profile					
	Exon	Forward	Reverse	Product length	ID	D	A	E	C	FE
E2F-1*										
DNA-binding domain	3	ccc cca gcc ccc atc atc ct	ctt ctg cac ctt cag cac ct	248 bp	5 min, 95 °C	45 s, 94 °C	35 s, 61 °C	35 s, 72 °C	30	5 min, 72 °C
Transactivation domain	7a	ccc ctg cct tcc tcc ctg ct	ctg atg ccc tcg ccc tcc tc	257 bp	5 min, 95 °C	45 s, 94 °C	35 s, 58 °C	30 s, 72 °C	30	5 min, 72 °C
	7b	gcc ttt ccc cac ccc acg a	gcc aga ccc cag agc tag aa	267 bp	5 min, 95 °C	45 s, 94 °C	35 s, 58 °C	30 s, 72 °C	30	5 min, 72 °C
mRNA	3–5	ggg gga gaa gtc acg cta tg	cac ggc ttg gag ctg ggt ct	463 bp	5 min, 95 °C	45 s, 94 °C	50 s, 58 °C	55 s, 72 °C	28	5 min, 72 °C
PCNA										
mRNA	1–4	gaa cct cac cag tat gtc ca	cag ctt cct cct ctt tat cg	373 bp	5 min, 95 °C	45 s, 94 °C	50 s, 58 °C	55 s, 72 °C	28	5 min, 72 °C

ID, initial denaturation; D, denaturation; A, annealing; E, extension; C, cycles, FE, final extension.
* Amplimer design is based on the E2F-1 sequence, GenBank accession number: U47675-7.

Method

PCR reactions were performed in 30 μl containing 10 mM Tris-HCl, pH 8.8, 50 mM KCl, 1.5 mM $MgCl_2$, 200 μ*M* of each dNTP (dATP, dCTP, dGTP and dTTP), 400 μ*M* *E2F-1* primers, 20 μ*M* *β-actin* primers, 2 μl of the cDNA pool and 2 Units of Taq DNA polymerase (Advanced Biotechnology, AntiSel, Greece). The thermal cycle profile is shown in Table 2. PCR products were electrophoresed in 1.8% agarose gel and stained with ethidium bromide.

Control

To avoid possible RT-PCR intra-assay fluctuations that could affect the original transcript ratio (target vs. reference), twofold serial dilutions of cDNA solutions were employed in control amplifications. From these reactions a low number of PCR cycles was established for assessing RNA transcript ratios.

Evaluation

The net intensity of each band was evaluated using an image analysis system (Kodak, AntiSel, Greece). *E2F-1 (PCNA)* quantity was normalized by estimating the *E2F-1*/*β-actin* ratio (*PCNA*/*β-actin* ratio). *E2F-1 (PCNA)* mRNA levels were assessed by estimating the relative ratio between tumour and corresponding normal specimens [*E2F-1*/*β-actin* (Tumour):*E2F-1*/*β-actin* (Normal)] [*PCNA*/*β-actin* (Tumour):*PCNA*/*β-actin* (Normal)]. The variability of this ratio within 20 pairs of normal specimens was found to be $1.05 \pm 0.17 (0.97 \pm 0.13)$. *E2F-1* mRNA (*PCNA*) overexpression was scored when the tumour : normal ratio was ≥ 2.0.

Differential (D)-PCR

E2F-1 gene amplification was assessed with the D-PCR method, as previously described [38]. Briefly, a target *E2F-1* DNA fragment was co-amplified with a shorter reference DNA fragment of *IFN-γ*. The relative ratios of the amplified products in the tumour samples reflect the relative proportion of gene copies and are compared to the relative ratios of the corresponding normal tissue.

Primers

The primers used for amplifying *E2F-1* target DNA fragment were those used for the mutational analysis of exon 3 (Table 2).

Method

PCR reactions were performed in 30 μl containing 10 mM Tris-HCl, pH 8.8, 50 mM KCl, 1.5 mM $MgCl_2$, 0.1% Triton X-100, 200 μ*M* of each dNTP (dATP, dCTP, dGTP and dTTP), 200 μ*M* of each *E2F-1* primer, 200 μ*M* of each *IFN-γ* primer, 2 μl of the DNA pool and 2 Units of Taq DNA polymerase (Advanced Biotechnology, Gram, Athens, Greece). The thermal cycle profile comprised an initial denaturation at 95 °C for 5 min before the addition of Taq polymerase and was followed by 28 cycles of 40 s at 94 °C, 40 s at 53 °C and 40 s at 72 °C. PCR products were electrophoresed in 2% agarose gels stained with ethidium bromide.

Control

To avoid possible D-PCR intra-assay fluctuations that could affect the original gene ratio (target vs. reference), twofold serial dilutions of DNA solutions were employed in control amplifications. From these reactions a low number of PCR cycles was established for assessing gene ratios.

Evaluation

The net intensity of each band was assessed using an image analysis system (Kodak, AntiSel, Greece). *E2F-1* quantity was normalized by estimating the *E2F-1*/*IFN-γ* ratio. *E2F-1* gene copies were assessed by estimating the relative ratio between tumour and corresponding normal specimens [*E2F-1*/*IFN-γ* (Tumour):*E2F-1*/*IFN-γ* (Normal)]. The variability of this ratio in 20 pairs of normal specimens was found to be 1.02 ± 0.11. *E2F-1* gene amplification was scored when the tumour : normal ratio was ≥ 2.0.

Mutation analysis

We performed mutation screening of the DNA-binding (exon 3) and transactivation (exon 7) domains, which represent important *E2F-1* functional regions, on cDNA material from 79 informative cases. Because of the large size of exon 7, two sets of primers generating overlapping PCR fragments were designed for SSCP compatibility. PCR reactions were performed in 30 μl containing 10 mM Tris-HCl, pH 8.8, 50 mM KCl, 1.5 mM $MgCl_2$, 200 μM of each dNTP, 400 μM of each *E2F-1* primer (Table 2), 2 μl of DNA and 1 Unit of Taq DNA polymerase (Advanced Biotechnology, Gram, Greece). The thermal cycle profiles for all examined fragments are presented in Table 2. Initial screening was performed by SSCP [34] and samples that exhibited mobility shifts were then subjected to sequencing using the ABI PRISM BigDye Terminator Cycle Sequencing Kit (Applied Biosystems, Vamvakas, Greece). Samples were run on an ABI 377 sequencer (Applied Biosystems, Vamvakas, Greece).

Kinetic parameters and ploidy status of the tumours

The information concerning the kinetic parameters (Proliferative index (PI), estimated by Ki-67 immunohistochemistry using the MIB-1 antibody and apoptotic index (AI), estimated by TUNEL assay) and

ploidy status, were acquired from our previous report [35] and are presented in Table 1.

pRb-p53-MDM2 protein network status

The alterations of the pRb/p53/MDM2 network were obtained from our previous studies [35,36] and are presented in detail in Table 1.

Statistical analysis

The association of E2F-1 immunoreactivity between normal and tumour areas, with the pathological parameters of histology and lymph node invasion, and with the CBP, pRb, p53, MDM2 and ploidy status were assessed using the *t*-test. The correlation between E2F-1 immunoreactivity and tumour stage was tested by analysis of variance (ANOVA). The relationship of E2F1 immunostaining with PI was examined with the parametric Pearson test, whereas its association with AI and GI was evaluated with the non-parametric Spearman test. Survival analysis was carried out according to the Kaplan–Meier methodology and log-rank test (univariant analysis) and Cox regression analysis (multivariate analysis). All tests were performed with the SPSS10 statistical package (SPSS Inc., Chicago, IL, USA). The statistical associations were considered significant when the p-value was <0.05.

Results

E2F-1 status and relationship with the clinicopathological parameters of the tumours (Tables 1 and 3)

E2F-1 protein analysis

Immunohistochemical analysis E2F-1 protein status was assessed as the percentage of stained tumour cells. E2F-1 was expressed both in normal lung parenchyma (Figure 1AI) and tumour areas (Figure 1AII). E2F-1 immunoreactivity ranged from 19% to 92% of the tumour cells, with a mean value of $45.7\% \pm 14.9\%$ (Table 1). The percentage of stained cells in the tumour region was significantly higher than in the corresponding normal epithelium (mean value: $12.1\% \pm 2.3\%$) ($p < 0.001$ by *t*-test analysis). In the normal lung parenchyma, E2F-1 staining was detected in the bronchial epithelium, mainly the basal cells, and in the pneumocytes of the alveoli. E2F-1-stained stromal cells were also observed (Figure 1AI). E2F-1 protein expression was significantly greater in squamous cell carcinomas (SCCs) than in adenocarcinomas (ADCs) ($p < 0.001$ by *t*-test analysis, Table 3). Correlation with lymph node status and disease stage did not reveal any further significant findings.

Western blot analysis The immunohistochemical findings were confirmed by western blotting, which showed a band of approximately 60 kDa in all the matched normal-tumour samples examined (Figure 2AI). All tumour areas expressed higher levels of E2F-1 than their normal counterparts. Densitometry analysis showed that the tumour to normal (T/N) ratio ranged between 2.5 to 3.7.

Table 3. Statistical analysis of E2F expression with clinicopathological data, pRb, p53 and MDM2 status

		N	E2F mean value	*p*
Histology	ADCs	37	38.5 ± 12.7	<0.001[a]
	SCCs	37	50.2 ± 12.2	
Ploidy	Aneuploid	42	50.0 ± 14.9	0.02[a]
	Diploid	32	41.8 ± 14.3	
Lymph node invasion	Yes	45	46.4 ± 14.6	0.663[a]
	No	35	44.9 ± 15.6	
Tumour stage	I	30	44.3 ± 16.1	0.570[b]
	II	27	45.1 ± 13.3	
	III	21	48.7 ± 15.7	
pRb status	Aberrant	32	50.0 ± 13.3	0.033[a]
	Normal	47	42.8 ± 15.3	
p53 status	Positive	45	49.2 ± 13.4	0.017[a]
	Negative	34	41.2 ± 15.7	
MDM2 status	Positive	52	48.6 ± 16.0	0.016[a]
	Negative	27	40.2 ± 10.8	
pRb/p53/ MDM2 status	Normal	12	39.6 ± 11.2	0.036[c]
	Full abnormal	24	52.9 ± 13.2	

[a] *t*-test analysis.
[b] ANOVA.
[c] Bonferroni analysis.

E2F-1 cDNA analysis

Comparative RT-PCR analysis E2F-1 cDNA analysis revealed that the majority of the cases (65/79, 82%) with E2F-1 protein overexpression demonstrated higher mRNA levels in the tumour area than in the corresponding adjacent normal tissue (Figure 2BI). In these samples the relative ratio ranged between 2.6 and 6.0, compared to the normal ratio of 1.05 ± 0.17.

Sequencing Mutation analysis of the DNA-binding and transactivation domains revealed that in two cases (2/79) point mutations were expressed (Table 1). In both cases, mutations were present in the transactivation domain: one was the previously reported polymorphism Gly393Ser (case 19) [31], whereas the other, Glu371Asp, was tumour-specific (case 47) (Figure 3C). Of note, in case 47 the tumour-specific mutation was accompanied by increased protein levels and immunohistochemical E2F-1 positivity (64%), although the mRNA levels were normal and there was no gene amplification, as estimated by differential PCR.

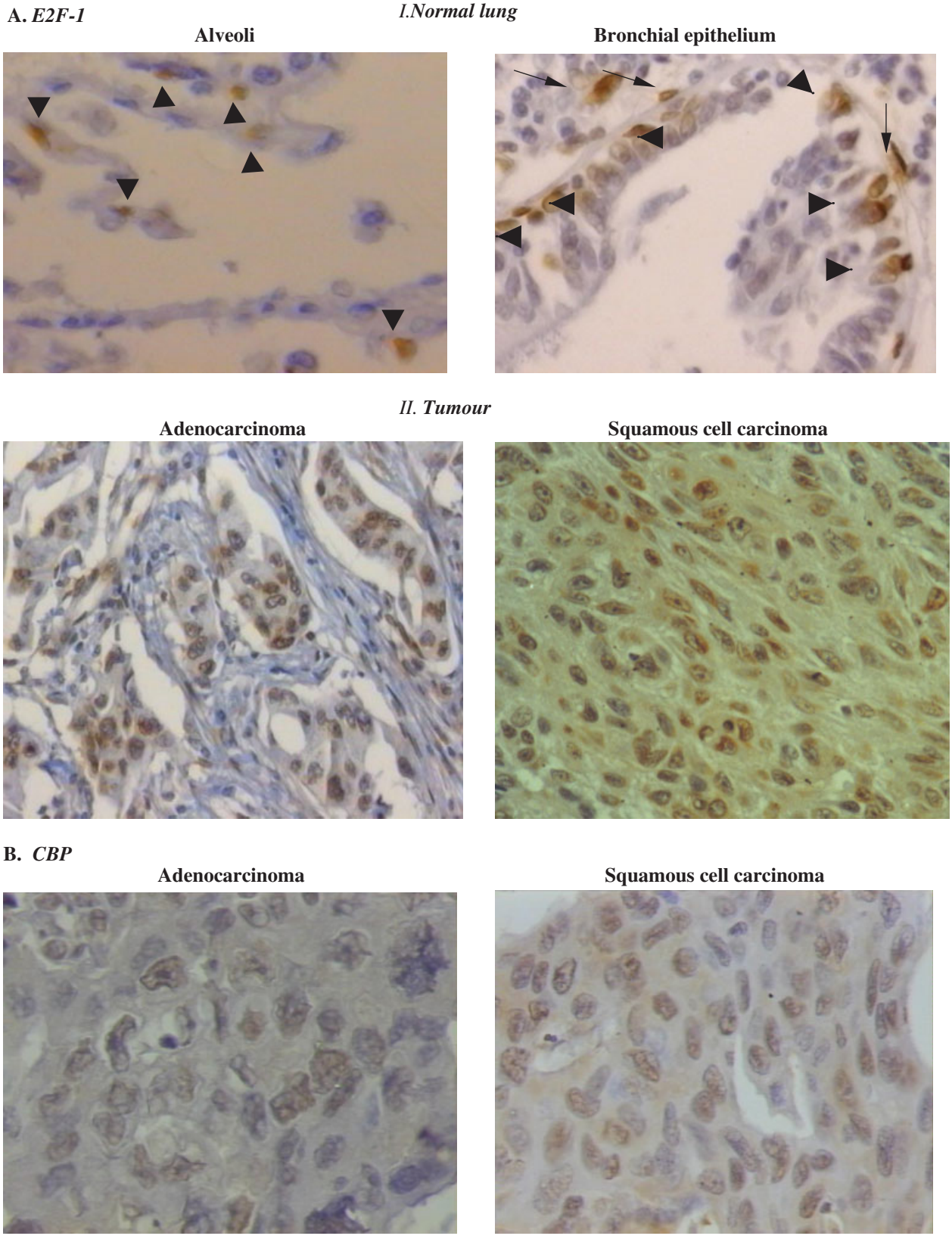

Figure 1. Representative immunohistochemical results. (AI) Normal lung tissue: in the alveoli, pneumonocytes with E2F-1 immunoreactivity are indicated by arrowheads. In the normal bronchial epithelium, basal cells with E2F-1 immunopositivity are shown by arrowheads, whereas E2F-1-positive stromal cells are indicated by arrows (×630). (AII) Lung adenocarcinoma (case 26) and squamous cell lung carcinoma (case 20) with nuclear E2F-1 immunoreactivity (50% and 53%, respectively) (×400). Streptavidin–biotin peroxidase technique with 'KH95' anti-E2F-1 antibody and haematoxylin counterstain. (B) Adenocarcinoma (case 8) and squamous cell lung carcinoma (case 7) with nuclear CBP immunoreactivity (60% and 70%, respectively) (×400). Streptavidin–biotin peroxidase technique with 'C-1' anti-CBP antibody and haematoxylin counterstain

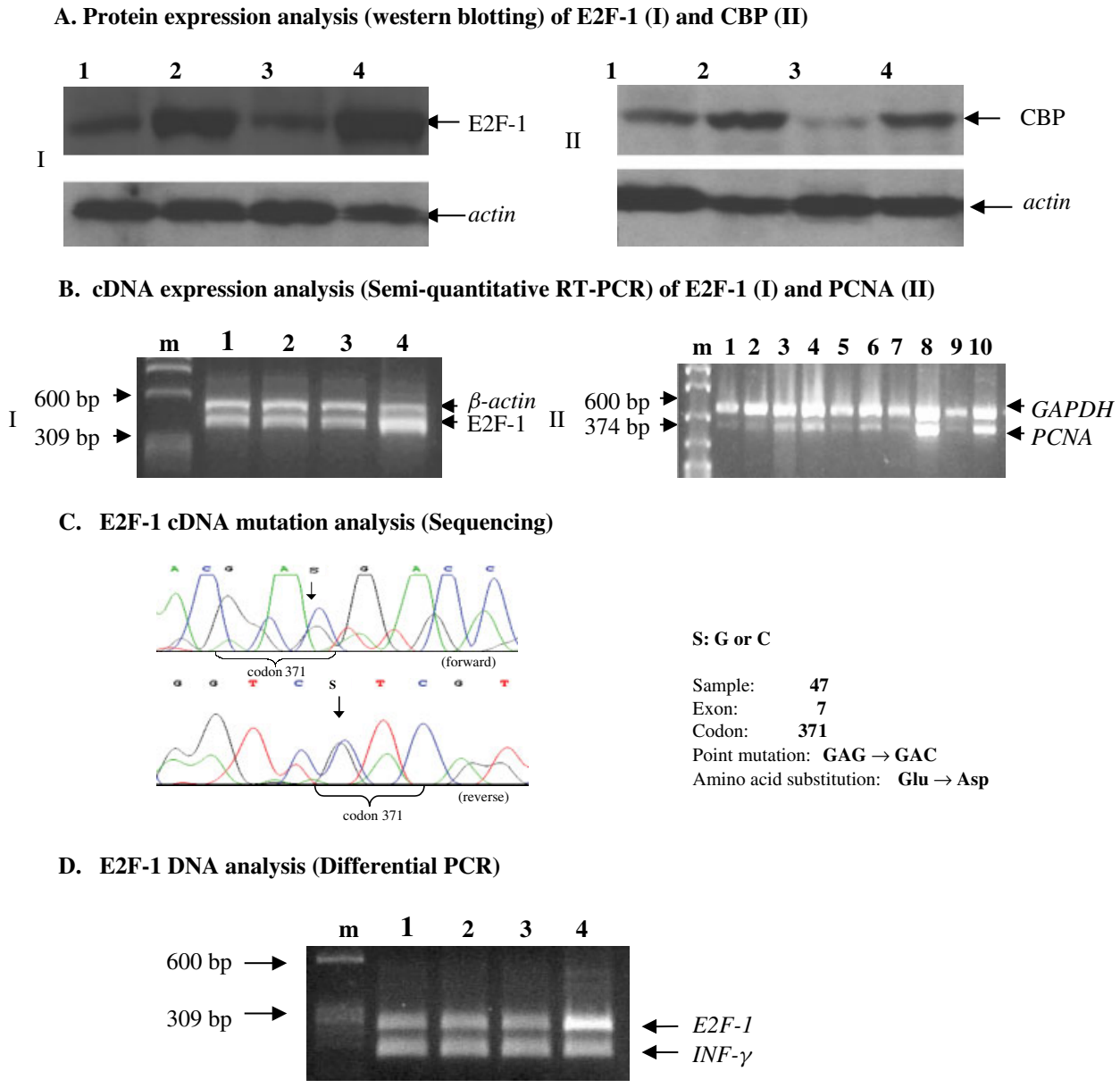

Figure 2. Representative results of the molecular analysis. (A) Results of the western blotting analysis of E2F-1 (I) and CBP (II) proteins for matched normal-tumour cases (57 and 58, and 21 and 22, respectively). Equal loading of total protein extracts was verified by actin western blotting. (BI) Results of the semi-quantitative multiplex RT-PCR for evaluation of the *E2F-1* mRNA (cDNA). **m**, ΦX174/HaeIII DNA ladder; lanes **1** and **2**, matched normal-tumour case (sample 16) with *E2F-1* mRNA normal expression; lanes **3** and **4**, matched normal-tumour case (sample 17) with *E2F-1* mRNA overexpression. (BII) Same analysis for PCNA. **m**, pBR322/MspI DNA ladder; lanes **1** and **2**, matched normal-tumour case (sample 18); lanes **3** and **4**, matched normal-tumour case (sample 1); lanes **5** and **6**, matched normal-tumour case (sample 3); lanes **7** and **8**, matched normal-tumour case (sample 47); lanes **9** and **10**, matched normal-tumour case (sample 53) with increased PCNA mRNA expression. (C) Representative automated sequencing in a squamous cell lung carcinoma (case 47) with SSCP mobility shifts in exon 7. The *E2F-1* mutation is located at codon 371 and changes GAG (E) to GAC (D). In this specific case the E2F-1 status was: immunohistochemical evaluation 64%, western blotting evaluation 2.5-fold above the E2F-1 protein level of the normal tissue, normal mRNA levels, no gene amplification; immunohistochemical evaluation of pRb, p53 and MDM2 was aberrant, positive and positive, respectively; the kinetic parameters were PI 54.4%, AI 0.5% and GI 108.8. (D) Representative results of the differential PCR for assessing the *E2F-1* gene amplification. **m**, ΦX174/HaeIII DNA ladder, lanes **1** and **2** and **3** and **4**: matched normal-tumour cases (samples 38 and 39, respectively) with *E2F-1* normal diploid gene status and *E2F-1* gene amplification, respectively

Estimation of E2F-1 levels in individual tumour and normal cells

In vivo studies which employ homogenized material (protein extracts or total mRNA) for quantitative analysis have the disadvantage of stromal cell contamination, which influences the exact assessment of the expression levels of a given molecule in individual cells. Based on the matched normal-tumour mRNA and protein analysis results we can estimate the individual E2F-1 tumour to normal cell (T/N) ratio with the following mathematical formula:

$$r = \frac{a \cdot P_T \cdot k \cdot A_N + (1 - a) \cdot P_N \cdot A_N}{P_N \cdot A_N}$$

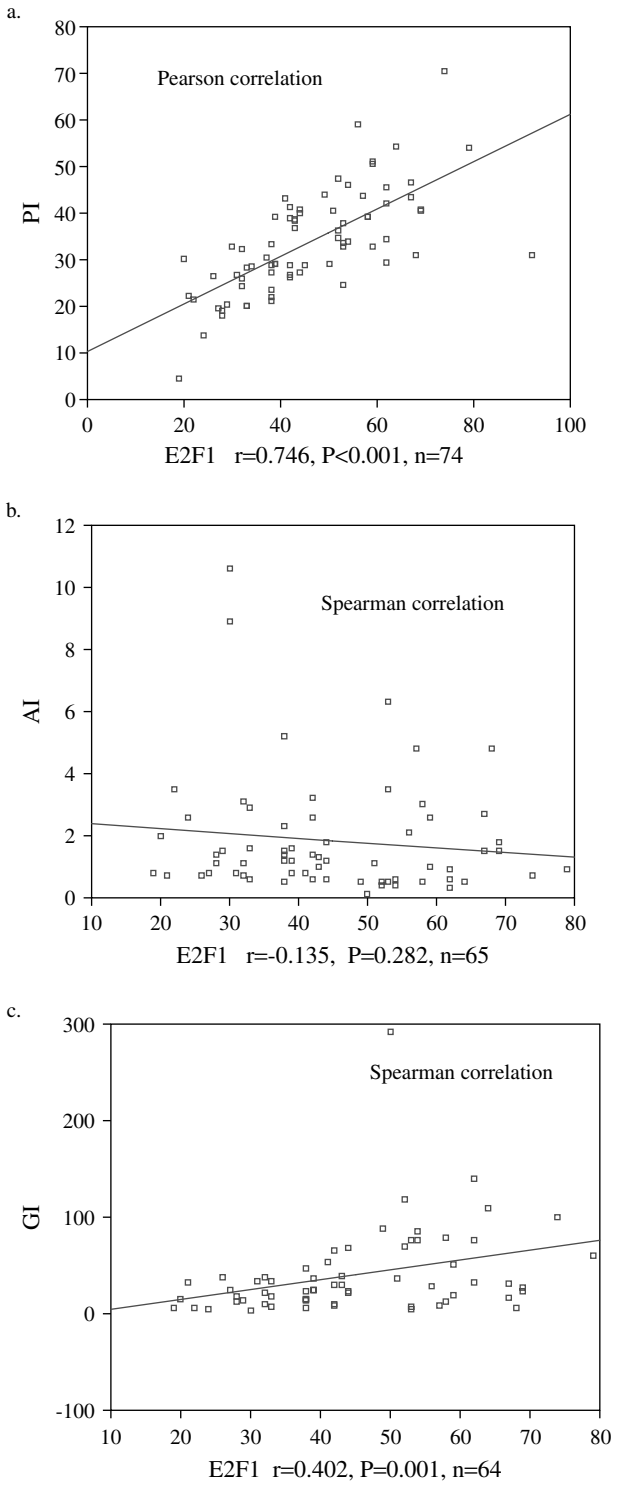

Figure 3. Diagrams (scatter plot and linear regression fit line) demonstrating the correlation between E2F-1 percentage and PI (a), AI (b) and GI (c)

where:

r: (estimated amount of expression product [E2F-1 mRNA or protein] in tumour sample)/(estimated amount of expression product [E2F-1 mRNA or protein] in adjacent normal sample);
a: percentage of tumour cells in cancerous area;
A_N: amount of expression product (E2F-1 mRNA or protein product) per normal cell;
k: (amount of expression product [E2F-1 mRNA or protein] in individual tumour cell)/(amount of expression product [E2F-1 mRNA or protein] in a normal cell)$= A_T/A_N$, and as a consequence:

$$A_T = k \cdot A_N$$

P_N: percentage of positive normal cells;
P_T: percentage of positive tumour cells.

Parameter k is the requested value. Values for P_N and P_T can be obtained from IHC analysis, while r values represent results either from comparative RT-PCR or western blot analysis in matched tumour-normal samples. Parameter A_N is deduced from the equation. The main difficulty in employing the above equation is obtaining the value a.

In the case of RT-PCR analysis, k values can be obtained, because parameter a can be estimated by microscopic evaluation of a 5 μm section. Then at least two serial 10 μm sections are adequate for mRNA extraction. More specifically, tumour samples for comparative RT-PCR analysis consisted of approximately 90% tumour cells ($a = 0.9$). Taking into consideration that P_T and P_N values range from 19% to 92% and 10% to 15%, respectively, and r ranges from 2.6- to 6.0-fold increase, k has a value between 2.0 and 4.2. This means that the individual tumour cells have 2.0- to 4.2-fold higher E2F-1 mRNA levels than normal.

However, in western blot analysis, a cannot be easily evaluated, due to the difficulty in determining the percentage of tumour cells in the tissue sample required for adequate protein extraction for this kind of analysis.

On the other hand, this mathematical expression can be easily applied in cell cultures ($a = 1$), which represent a homogeneous system and where the P_T and P_N values are equal to 1.

E2F-1 DNA analysis

The possibility of gene amplification was investigated with the D-PCR analysis. E2F-1 gene amplification was found in seven out of 79 informative cases (9%) (Table 1, Figure 2D). In the above specimens the relative ratio varied between 2.3 and 4.2, whereas the values of the corresponding normal tissue were 1.02 ± 0.11 (Table 1, Figure 3D). All of the specimens with gene amplification demonstrated high E2F-1 staining indexes and increased E2F-1 protein and mRNA levels (Table 1).

Relationship of E2F-1 status to the kinetic parameters (Figure 3) and ploidy status of the tumours (Table 3)

Proliferation index (PI) ranged from 4.6% to 70.4%, with a mean value of $35.2\% \pm 11.3\%$ (Table 1). A strong positive correlation was observed between E2F-1 immunoreactivity and proliferation index (correlation coefficient factor r: 0.746, $p < 0.001$ by Pearson correlation) (Figure 3a).

Apoptotic index (AI) ranged from 0.1% to 10.6%, with a mean value of $2.04 \pm 2.06\%$ (Table 1). No association was found between E2F-1 status and apoptotic index of the tumors ($r = -0.135, p = 0.282$ by Spearman correlation) (Figure 3b).

Growth index, defined as the ratio of PI to AI, was positively correlated with E2F-1 protein expression ($r = 0.402, p = 0.001$ by Spearman correlation) (Figure 3c).

Ploidy analysis revealed 46 aneuploid carcinomas out of 80 examined (58.0%). The aneuploid tumours had significantly higher percentages of E2F-1 positive cells than the diploid ($p = 0.02$ by t-test analysis).

Finally, due to the wide range of proliferation index (4.6–70.4%) detected in our tumour samples, we decided to assess the increase at transcriptional level of the PCNA marker, which peaks during S phase. Semi-quantitative RT-PCR analysis showed that in tumour samples, PCNA levels were increased between 2.4- and 5.3-fold compared to adjacent normal tissue (Figure 2BII). These levels of increase are similar to that found for E2F-1.

CBP status

Immunohistochemical analysis CBP protein status was assessed as the percentage of stained tumour cells. Staining was mainly nuclear, but faint cytoplasmic reactivity was also observed in certain cases. The faint cytoplasmic activity may be due to histone acetylo-transferase activity (HAT) of CBP [39]. CBP was expressed both in normal lung parenchyma and tumour areas (Figure 1B). CBP immunoreactivity ranged from 60% to 80% of the tumour cells, with a mean value of $65.3 \pm 7.7\%$ (Table 1). The percentage of stained cells in the tumour was significantly higher than in the corresponding normal epithelium (mean value: $15.4 \pm 3.1\%$) ($p < 0.001$ by t-test analysis). In the normal lung parenchyma, CBP staining was detected in the bronchial epithelium, mainly the basal cells, and in the alveolar pneumocytes. There was no significant difference in CBP protein expression between squamous cell carcinomas and adenocarcinomas (Table 3). Correlation with lymph node status and disease stage did not reveal any further significant findings.

Western blot analysis The immunohistochemical findings were confirmed by western blotting, which showed a band of approximately 265 kDa in all the matched normal-tumour samples examined (Figure 2AII). All tumour areas expressed higher levels of CBP than their normal counterparts. Densitometry analysis showed that the tumour to normal (T/N) ratio ranged between 2.3 and 3.5.

Relationship with the pRb-p53-MDM2 network (Table 3)

The pRb-p53-MDM2 network status was obtained from our previous studies [35,36]. Increased E2F-1 staining was positively correlated with abnormal pRb expression ($p = 0.033$ by t-test analysis), p53 immunoreactivity ($p = 0.017$ by t-test analysis) and MDM2 staining ($p = 0.016$ by t-test analysis). Moreover, examining the status of E2F-1 in the cases with normal and defective pRb-p53-MDM2 networks, we found that only the full abnormal pattern [pRb(Ab)/p53(P)/MDM2(P)] demonstrated significantly higher E2F-1 levels than normal ($p = 0.036$ by Bonferroni analysis).

Outcome and survival analysis (Table 4, Figure 4)

Survival analysis was conducted with 85 patients because no follow-up information was available for two cases. During the course of the study (maximal follow-up 60 months, median follow-up 25 months), 44 failures and 41 censored cases were recorded. Three patients who died during surgery were excluded. In the remaining cases with follow-up data, E2F-1 was informative in 77 samples. The use of the E2F1 median value as a cut-off point revealed a significant association between increased E2F-1 immunoreactivity and poor patient outcome ($p = 0.033$ by Cox regression and $p = 0.014$ by Kaplan–Meier methodology) (Table 4). Particularly, the group with E2F-1 values less than the E2F-1 median value (43%) included 39 patients; 24 of them were censored and 15 died (mean and median survival time 29 and 28 months, respectively). The other group with high E2F-1 values consisted of 38 patients; 14 were censored and 24 died (mean and median survival time 21 and 18 months, respectively). Moreover, as previously reported in the same series of patients [35], pRb, p53, MDM2 status and kinetic parameters were not significantly prognostic.

Discussion

The E2F-1 transcription factor is considered to be the 'final frontier' of the G1 to S phase boundary. Many

Table 4. Survival analysis

Kaplan–Meier method	**Log-rank test**	
	Statistic	***p***
	6.00	0.014
	20.07	<0.001
	9.56	0.008
Cox-regression analysis	**Backward stepwise method**	
	Wald test	***p***
	4.55	0.033
	10.35	0.001

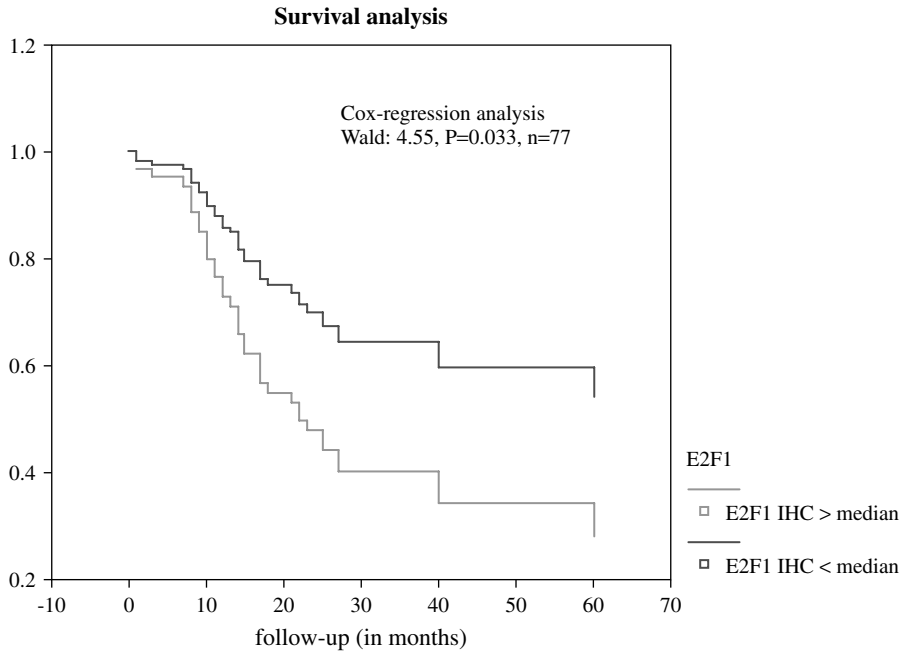

Figure 4. Survival curves related to E2F-1 expression, from 77 non-small cell lung cancer patients. Increased E2F-1 expression was significantly associated with poor survival ($p = 0.033$ by Cox regression analysis)

upstream stimulatory and inhibitory signals converge on the pRb-E2F-1 complex, which orchestrates early cell cycle progression. *In vitro* studies have indicated that E2F-1 could function either as an oncogene or as a tumour suppressor gene [1,2,7,17,18]. This controversy also seems to exist in the few reported *in vivo* studies [29,31].

In the present study, E2F-1 protein levels in the tumour were significantly higher than in the corresponding adjacent normal epithelium, as assessed by immunohistochemistry and western blotting ($p < 0.001$). Interestingly, E2F-1 overexpression was associated with increased levels of its co-activator CBP. CBP and its counterpart p300 are closely related transcriptional co-activators, which stimulate the activity of a wide spectrum of transcription factors [40]. They both possess histone acetylase activity [18]. *In vitro* experiments have demonstrated that defective interaction of E2F-1 with CBP leads to reduced transactivation activity of E2F-1 [41]. Histologically, squamous cell lung carcinomas exhibited significantly higher percentages of E2F-1-positive cells than adenocarcinomas (Table 3), reflecting the different biological profiles of these NSCLC histological subtypes [42]. Increased E2F-1 protein levels were associated in the majority of the cases (82%) with higher than normal *E2F-1* mRNA levels in the tumour, whereas the frequency of *E2F-1* gene amplification was relatively low (9%, Table 1). It is of note that the chromosomal region 20q, which contains the *E2F-1* gene, is a frequent locus of gains, as demonstrated by several groups [43–45]. Thus, in certain cases, the observed *E2F-1* gene amplification could be the result of a broader gain in chromosome locus 20q, instead of a localized amplification. Our findings are in accordance with those of Suzuki *et al*. in gastrointestinal carcinomas, where E2F-1 protein overexpression was mainly associated with increased mRNA levels, rather than gene amplification, which was seen in 11% of the cases examined [32]. Taken together, these data suggest that deregulated *E2F-1* mRNA synthesis is a main mechanism of E2F-1 protein overexpression in certain neoplasms. Apart from *E2F-1* mRNA synthesis modulation [14,46], additional and frequently overlapping mechanisms regulating the levels and activity of E2F-1 include degradation by the ubiquitin/proteosome pathway [47], post-translational modifications such as phosphorylation [48] and acetylation [49] and protein–protein interactions [2,50].

The information concerning the control of E2F-1 at the level of transcription is rather limited. The E2F-1 promoter harbours potential binding sites for Sp-1, ATF, E4F, NF-κB and members of the E2F family [14,46]. While the functional significance of this organization is uncertain, it is noteworthy that E2F-1 can positively autoregulate its own transcription and that pRb, in addition to regulating E2F-1 activity, may directly or indirectly interact with Sp-1 and ATF-2 [51–53]. Furthermore, biochemical evidence presented by Weintraub and colleagues suggests that the pRb-E2F complexes are not inert, but serve as potent transcriptional repressors, by recruiting histone deacetylase and blocking the access of E2F-1 co-activator CBP [2,54]. Thus, it is possible that the balance between E2F-1 (and probably E2F-2 and E2F-3) [14] and pRb status determines, to a significant extent, E2F-1 transcription. Our finding that carcinomas with increased E2F-1 positivity were associated with aberrant pRb expression ($p = 0.03$, Table 3) and high CBP levels might support this notion.

This result, however, raises the question of how E2F-1 escapes degradation by the ubiquitin–proteosome pathway in those cases with aberrant/absent pRb expression, since the latter has the ability to protect E2F family members from this process [47]. One possible explanation is epigenetic abnormalities in the ubiquitin–proteosome pathway. Dysregulated proteolysis of cell cycle regulators, including p53, p27 and cyclins D1, E and B, is frequently observed in cancer [55]. On the other hand, other mechanisms of stabilization seem to exist in the cell, because expression of the adenovirus E1A protein, which blocks pRb, also leads to stabilization of E2F-1 [47,56]. Even though aberrant/absent pRb expression can explain deregulation of E2F-1 transcription in a subset of the carcinomas examined, the observation that cases with normal pRb expression were accompanied by increased *E2F-1* mRNA levels (Table 1) adds a further level of complexity to the E2F-1-pRb interplay. Alternative scenarios for pRb inactivation may be involved in these cases, such as hyperphosphorylation by cyclin D1 or inactivation of p16, which are frequently deregulated in NSCLCs [42,57]. Eleven cases demonstrated a high percentage of E2F-1 positive cells with normal *E2F-1* mRNA levels (Table 1). It appears that in these tumours, E2F-1 protein overexpression is not due to deregulation of transcription, but rather to aberrations at the post-transcriptional level, and most probably to defects of the degradation machinery. This discordance between E2F-1 protein and mRNA levels has been found in normal cycling cells [58] and during myoblast differentiation [59], suggesting that degradation of E2F-1 plays a significant role in regulating its activity.

Sequence analysis revealed two missense point mutations, both in the E2F-1 transactivation domain. One was the previously reported polymorphism at codon 393, consisting of a Gly to Ser substitution (case 19, Table 1) [31], whereas the other, a Glu to Asp substitution (case 47, Table 1), was tumour-specific and was located at codon 371, the first reported *E2F-1* tumour-specific mutation. Nakamura *et al*. failed to detect any mutation in the pRb-binding domain of E2F-1 in a variety of carcinomas, including lung [60]. The significance of mutation Glu371Asp is ambiguous. Codon 371 lies between the MDM2-binding domain of E2F-1 and serine 375 (Figure 1), whose phosphorylation by cyclin A-cdk2 and cyclin A-cdc2 downregulates E2F-1 transactivation potential [61–63]. Thus, one possibility is that this mutation interferes with phosphorylation of Ser 375 and hence upregulates the activity of E2F-1.

The most important findings of the present study are that the carcinomas with increased E2F-1 positivity have significantly raised growth indexes (Figure 3c) and were associated with poor patient outcome. E2F-1 status was found to be an independent prognostic factor by Cox regression analysis (Figure 4). These novel results suggest that E2F-1 status may be a useful prognostic marker. Further analysis of our data revealed that the main determinant of this positive association with growth was the parallel increase between E2F-1 staining and proliferation, whereas apoptosis was not influenced by E2F-1 status (Figure 4a, b). A similar correlation between E2F-1 expression and proliferation was reported in breast carcinomas and neuroendocrine lung tumours by Zhang *et al*. [29] and Eymin *et al*. [34], respectively. Eymin *et al*. did not assess the relationship of E2F-1 with the apoptotic index, although they demonstrated an increased Bcl-2: Bax ratio, implying a pro-apoptotic deregulation [29,34]. Interestingly, and in contrast to our findings, Eymin *et al*., in a series of only 17 NSCLCs, detected E2F-1 immunohistochemically in only one sample and failed to identify E2F-1 in normal lung epithelium and stromal cells [34]. Although this could be explained by the small number of cases studied, it does not provide a convincing explanation for the complete absence of E2F-1 reactivity in adjacent normal tissue, which is expected in renewal epithelia [29].

The absence of correlation with apoptosis in our series and the *in vitro* reports, which implicate E2F-1 in inducing the apoptotic process [24,28,64–66], prompted us to investigate its relationship with the status of p53 protein, the main E2F-1 mediator of programmed cell death [15,67,68], and MDM2 protein, the principal p53 antagonist [69,70]. Interestingly, we found that the carcinomas with increased E2F-1 expression frequently had *p53* alterations ($p = 0.017$, Table 3) and showed high MDM2 levels ($p = 0.016$, Table 3). Besides its ability to bypass the functions of wt p53 [70], MDM2 has a profound impact on E2F-1 activity by converting it from a negative to a positive regulator of cell cycle progression [10,70,71]. Although deregulation of the p53-MDM2 duet can explain to a significant extent the lack of correlation between E2F-1 overexpression and apoptosis in our series, other p53-independent pathways involved in E2F-1-mediated apoptosis may be defective and could apply in the cases with a normal p53-MDM2 pathway [72,73]. A recent report by Stiewe and Putzer implicates the p53 homolog p73 in such a process [74]. Finally, we observed significantly higher E2F-1 staining indexes in the aneuploid than in the diploid tumours ($p = 0.02$, Table 3), which probably reflects the impact of E2F-1 overexpression on the proliferative activity of the cancer cells. Shortening of the G1 phase and inappropriate entry into S phase results in genetic instability [75]. Moreover, deregulation of the E2F-1-pRb pathway may have consequences beyond the G1 phase, because an interplay between E2F-1, cyclin A-cdk2, anaphase promoting complex (APC) and cyclin B-cdc2 has recently been documented [76]. Deregulation of this link may lead to abnormal chromosome segregation.

In conclusion, our results suggest that E2F-1 overexpression may contribute to the development of NSCLCs by promoting proliferation, particularly where there is a defect in the pRb/p53/MDM2 network. Based on our findings and those reported by

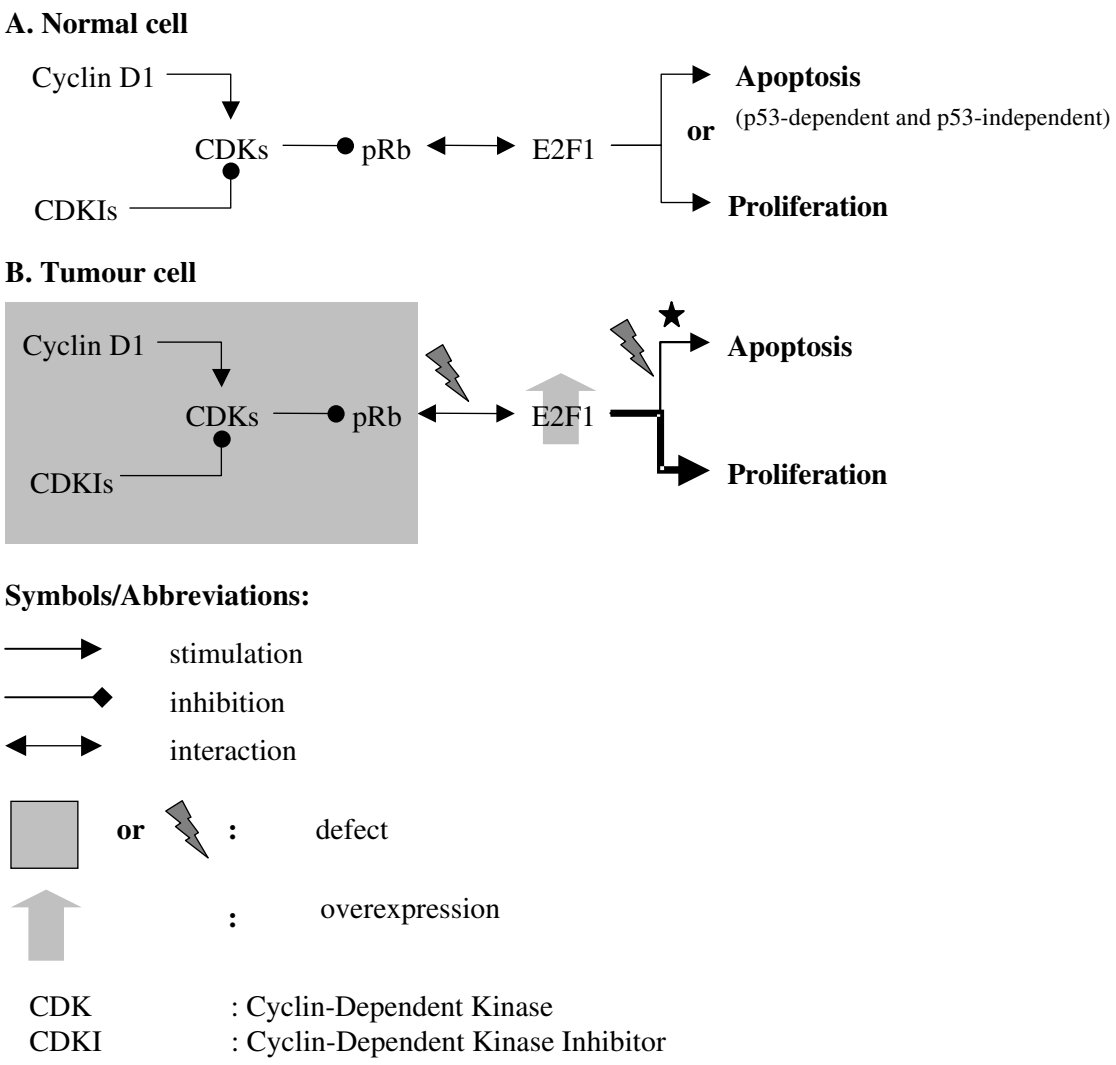

Figure 5. A hypothetical model showing the alterations of the pRb/E2F-1 and p53/MDM2 pathways in tumour progression of a subset of NSCLCs. (A) The pRB/E2F-1 pathway in a normal cell. At present [2] it is not clear which regulatory network effects determine E2F-1-induced proliferation or E2F-1-induced apoptosis in a normal cell. (B) In a tumour cell, deregulation of the pRb-E2F-1 network stimulates p53-dependent and/or -independent apoptotic pathways [77]. This effect causes a survival pressure for the cell to eliminate, directly (via *p53* mutations) and/or indirectly (MDM2 overexpression), the p53-dependent apoptotic response [78], while defective p53-independent apoptotic mechanisms can also cooperate [74]. Then, in the background of a defective pRb-p53-MDM2 network, released E2F-1 promotes proliferation [79]

others in transgenic models [74,77–79], we propose the following hypothesis (Figure 5). In a subset of NSCLCs, deregulation of the pRb-E2F-1 pathway triggers a compensatory p53-dependent and/or independent apoptotic response, in order to eliminate the pRb defective cell [77]. This reaction regulates a survival 'pressure' for the cell to neutralize the apoptotic response by obviating directly (mutations) and/or indirectly (MDM2 overexpression) the p53-dependent functions [78], while defective p53-independent apoptotic mechanisms can also be involved [74]. Released from the surveillance of pRb and with its apoptotic capabilities crippled, E2F-1 then promotes tumour progression [79].

Acknowledgements

We would like to thank Dr P. Kanavaros and Dr T. Liloglou for their valuable help and criticism during the preparation of this work. This study was funded in part by Greek GSRT research programme EPET 11 97, EKBAN2-112, METRO 1.2, 70/3/4396, and National and Capodistrian University of Athens research programme ELKE, 70/4/4591, 21/11/00.

References

1. Dyson N. The regulation of E2F by pRb-family proteins. *Genes Dev* 1998; **12**: 2245–2262.
2. Black RA, Azizkhan-Clifford J. Regulation of E2F: a family of transcription factors involved in proliferation control. *Gene* 1999; **237**: 281–302.

3. Hesketh R. E2F1 *The Oncogene and Tumor Suppressor Gene: Factsbook* (2nd edn). Academic Press: London, 1997; 425–427.
4. Huber HE, Goodhart PJ, Huang PS. Retinoblastoma protein reverses DNA bending by transcription factor E2F. *J Biol Chem* 1994; **269**: 6999–7005.
5. Bandara LR, Lam W-FE, Sorensen TS, Zamanian M, Girling R, La Thangue NB. DP-1: a cell cycle-regulated and phosphorylated component of transcription factor DRTF1/E2F which is functionally important for recognition by pRb and the adenovirus E4 orf 6/7 protein. *EMBO J* 1994; **13**: 3104–3114.
6. Helin K, Wu C-L, Fattaey A, *et al*. Heterodimerization of the transcription factors E2F-1 and DP-1 leads to cooperative transactivation. *Genes Dev* 1993; **7**: 1850–1861.
7. Muller H, Helin K. The E2F transcription factors: key regulators of cell proliferation. *Biochim Biophys Acta* 2000; **1470**: M1–M12.
8. Hagemeier C, Cook A, Kouzarides T. The retinoblastoma protein binds E2F residues required for activation *in vivo* and TBP binding *in vitro*. *Nucleic Acid Res* 1993; **21**: 4998–5504.
9. Pearson A, Greenblatt J. Modular organization of the E2F1 activation domain and its interaction with general transcription factors TBP and TFIIH. *Oncogene* 1997; **15**: 2643–2658.
10. Martin K, Trouche D, Hagemeier C, Sorensen TS, Lathangue NB, Kouzarides T. Stimulation of E2F1/DP1 transcriptional activity by mdm2 oncoprotein. *Nature* 1995; **375**: 691–694.
11. Lee CW, Sorensen TS, Shikama N, Lathangue NB. Functional interplay between p53 and E2F through co-activator p300. *Oncogene* 1998; **16**: 2695–2710.
12. Ross JF, Liu X, Dynlacht BD. Mechanism of transcriptional repression of E2F by the retinoblastoma tumor suppressor protein. *Mol Cell* 1999; **3**: 195–205.
13. Brehm A, Miska EA, McCance DJ, Reid JL, Bannister AJ, Kouzarides T. Retinoblastoma protein recruits histone deacetylase to repress transcription. *Nature* 1998; **391**: 597–601.
14. Neuman E, Flemington E, Sellers W, Kaelin W. Transcription of the E2F-1 gene is rendered cell cycle dependent by E2F DNA-binding sites within its promoter. *Mol Cell Biol* 1994; **14**: 6607–6615.
15. Bates S, Phillips AC, *et al*. P14ARF links the tumor suppressors RB and p53. *Nature* 1998; **395**: 124–125.
16. O'Connor DJ, Lam EW, Griffin S, *et al*. Physical and functional interactions between p53 and cell cycle co-operating transcription factors, E2F1 and DP1. *EMBO J* 1995; **14**: 6184–6192.
17. Yamasaki L. Balancing proliferation and apoptosis *in vivo*: the Goldilocks theory of E2F/DP action. *Biochim Biophys Acta* 1999; **1423**: M9–M15.
18. Harbour JW, Dean DC. The Rb/E2F pathway: expanding roles and emerging paradigms. *Genes Dev* 2000; **14**: 2393–2409.
19. Gala S, Marreiros A, Stewart GJ, Williamson P. Overexpression of E2F-1 leads to cytokine-independent proliferation and survival in the hematopoietic cell line BaF-B03. *Blood* 2001; **97**: 227–234.
20. Zhang SY, Liu SC, Johnson DG, Klein-Szanto AJP. E2F1 gene transfer enhances invasiveness of human head and neck carcinoma cell lines. *Cancer Res* 2000; **60**: 5972–5976.
21. Johnson DG, Cress WD, Jakoi L, Nevins JR. Oncogenic capacity of the E2F1 gene. *Proc Natl Acad Sci USA* 1994; **91**: 12823–12827.
22. Yamazaki L, Jaks T, Bronson R, Goillot E, Harlow E, Dyson NJ. Tumor induction and tumor atrophy in mice lacking E2F1. *Cell* 1996; **85**: 537–548.
23. Hunt KK, Deng J, Liu T-J, *et al*. Adenovirus-mediated overexpression of the transcription factor E2F-1 induces apoptosis in human breast and ovarian carcinoma cell lines and does not require p53. *Cancer Res* 1997; **57**: 4722–4726.
24. Field S, Tsai F-Y, Kuo F, *et al*. E2F-1 functions in mice to promote apoptosis and suppress proliferation. *Cell* 1996; **85**: 549–561.
25. Phillips AC, Bates S, Ryan KM, Helin K, Vousden H. Induction of DNA synthesis and apoptosis are separable functions of E2F-1. *Genes Dev* 1997; **11**: 1853–1863.
26. Shan B, Durfee T, Lee W-H. Disruption of Rb/E2F-1 interaction by single point mutations in E2F-1 enhances S-phase entry and apoptosis. *Proc Natl Acad Sci USA* 1996; **93**: 679–684.
27. Krek W, Xu G, Livingston D. Cyclin A-kinase regulation of E2F-1 DNA binding function underlies suppression of an S phase checkpoint. *Cell* 1995; **83**: 1149–1158.
28. Shan B, Lee W-H. Deregulated expression of E2F-1 induces S-phase entry and leads to apoptosis. *Mol Cell Biol* 1994; **14**: 8166–8173.
29. Zhang SY, Liu SC, Al-Saleem LF, *et al*. E2F-1: a proliferative marker of breast neoplasia. *Cancer Epidemiol Biomarkers Prev* 2000; **9**: 395–401.
30. Lai R, Medeiros LJ, Coupland R, McCourty A, Brynes RK. Immunohistochemical detection of E2F1 in non-Hodgkin's lymphomas: a survey of 124 cases. *Mod Pathol* 1998; **11**: 457–463.
31. Rabbani F, Richon VM, Orlow I, *et al*. Prognostic significance of transcription factor E2F-1 in bladder cancer: genotypic and phenotypic characterization. *J Natl Cancer Inst* 1999; **91**: 874–881.
32. Suzuki T, Yasui W, Yokozaki H, Naka K, Ishikawa T, Tahara E. Expression of the E2F family in human gastrointestinal carcinomas. *Int J Cancer* 1999; **81**: 535–538.
33. Volm M, Koomagi R, Rittgen W. Clinical implications of cyclins, cyclin-dependent kinases, RB and E2F1 in squamous-cell lung carcinoma. *Int J Cancer* 1998; **79**: 294–299.
34. Eymin B, Gazzeri S, Brambilla C, Brambilla E. Distinct pattern of E2F1 expression in human lung tumors: E2F1 is upregulated in small cell lung carcinoma. *Oncogene* 2001; **20**: 1678–1687.
35. Gorgoulis VG, Zacharatos P, Kotsinas A, *et al*. Altered expression of the cell cycle regulatory molecules pRb, p53 and MDM2 exert a synergetic effect on tumor growth and chromosomal instability in non-small cell lung carcinomas (NSCLC). *Mol Med* 2000; **6**: 208–237.
36. Gorgoulis VG, Zacharatos P, Kotsinas A, *et al*. Alterations of the p16-pRb pathway and the chromosome locus 9p21–22 in non-small-cell lung carcinomas: relationship with p53 and MDM2 protein expression. *Am J Pathol* 1998; **153**: 1749–1765.
37. Davis LG, Dibner MD, Battey JF. *Basic Methods in Molecular Biology*. Elsevier Science: New York, 1986;
38. Gorgoulis VG, Zacharatos P, Mariatos G, *et al*. Deregulated expression of c-mos in non-small cell lung carcinomas (NSCLCs). Relationship with p53 status, genomic instability and tumor kinetics. *Cancer Res* 2001; **61**: 538–549.
39. Mahlknecht U, Hoelzer D. Histone acetylation modifiers in the pathogenesis of malignant disease. *Mol Med* 2000; **6**: 623–644.
40. Snowden AW, Perkins ND. Cell cycle regulation of the transcriptional coactivators p300 and CREB binding protein. *Biochem Pharmacol* 1998; **55**: 1947–1954.
41. Trouche D, Cook A, Kouzarides T. The CBP co-activator stimulates E2F1/Dp1 activity. *Nucleic Acid Res* 1996; **24**: 4139–4145.
42. Sekido Y, Fong KM, Minna JD. Progress in understanding the molecular pathogenesis of human lung cancer. *Biochim Biophys Acta* 1998; **1378**: F21–F59.
43. Michelland S, Gazzeri S, Brambilla E, Robert-Nicoud M. Comparison of chromosomal imbalances in neuroendocrine and non-small-cell lung carcinomas. *Cancer Genet Cytogenet* 1999; **114**: 22–30.
44. Petersen S, Aninat-Meyer M, Schluns K, Gellert K, Dietel M, Petersen I. Chromosomal alterations in the clonal evolution to the metastatic stage of squamous cell carcinomas of the lung. *Br J Cancer* 2000; **82**: 65–73.
45. Luk C, Tsao M, Bayani J, Shepherd F, Squire JA. Molecular cytogenic analysis of non-small cell lung carcinoma by spectral karyotyping and comparative genomic hybridization. *Cancer Genet Cytogenet* 2001; **125**: 87–99.
46. Hsiao KM, McMahon SL, Farhham PJ. Multiple DNA elements are required for the growth regulation of the mouse E2F1 promoter. *Genes Dev* 1994; **13**: 1526–1537.
47. Hofmann F, Martelli F, Livingston DM, Wang Z. The retinoblastoma gene product protects E2F1 from degradation by the ubiquitin–proteasome pathway. *Genes Dev* 1996; **10**: 2949–2959.

48. Wang S, Nath N, Minden A, Chellappan S. Regulation of Rb and E2F by signal transduction cascades: divergent effects of JNK1 and p38 kinases. *EMBO J* 1999; **18**: 1559–1570.
49. Martinez-Balbas MA, Bauer UM, Nielsen SJ, Brehm A, Kouzarides T. Regulation of E2F1 activity by acetylation. *EMBO J* 2000; **19**: 662–671.
50. Stiegler P, Kasten M, Giordano A. The family of cell cycle regulatory factors. *J Cell Biochem (Suppl)* 1998; **31**: 30–36.
51. Lin S-Y, Black AR, Kostic A, Pajovic S, Hoover CN, Azizkhan JC. Cell cycle regulated association of E2F1 and SP1 is related to their functional interaction. *Mol Cell Biol* 1996; **16**: 1668–1675.
52. Udvadia A, Rogers KT, Higgins PDR, *et al*. Spl binds promoter elements regulated by the Rb protein and Spl stimulated transcription is stimulated by Rb coexpression. *Proc Natl Acad Sci U S A* 1993; **90**: 3265–3269.
53. Kim S-J, Wagner S, Liu F, O'Reilly MA, Robbins PD, Green MR. Retinoblastoma gene product activates expression of the human TGF-β2 gene through transactivation factor ATF-2. *Nature* 1992; **358**: 331–334.
54. Weintraub SJ, Prater CA, Dean DC. Retinoblastoma protein switches the E2F site from positive to negative element. *Nature* 1992; **358**: 259–261.
55. Sparato V, Norbury C, Harris AL. The ubiquitin–proteasome pathway in cancer. *Br J Cancer* 1998; **77**: 448–455.
56. Hateboer G, Kerkhoven RM, Shvarts A, Bernards R, Beijersbergen RL. Degradation of E2F by the ubiquitin–proteasome pathway, regulation by retinoblastoma family proteins and adenovirus transforming proteins. *Genes Dev* 1996; **10**: 2960–2970.
57. Mariatos G, Gorgoulis VG, Zacharatos P, *et al*. Expression of $p16^{INK4A}$ and alterations of the 9p21–23 chromosome region in non-small cell lung carcinomas: relationship with tumor growth parameters and ploidy status. *Int J Cancer* 2000; **89**: 133–141.
58. Leone G, DeGregori J, Yan Z, *et al*. E2F3 activity is regulated during the cell cycle and is required for the induction of S-phase. *Genes Dev* 1998; **12**: 2120–2130.
59. Martelli F, Livingston DM. Regulation of endogenous E2F1 stability by the retinoblastoma family proteins. *Proc Natl Acad Sci USA* 1999; **96**: 2858–2863.
60. Nakamura T, Monden Y, Kawashima K, Naruke T, Nishimura S. Failure to detect mutations in the retinoblastoma protein-binding domain of the transcription factor E2F-1 in human cancers. *Jpn J Cancer Res* 1996; **87**: 1204–1209.
61. Pepper DS, Keblusek P, Helin K, Toebes M, van der Eb AJ, Zantema A. Phosphorylation of a specific cdk site in E2F1 affects its electrophoretic mobility and promotes pRb-binding *in vitro*. *Oncogene* 1995; **10**: 39–48.
62. Dynlacht BD, Flores O, Lees JA, Harlow E, Zhu L. Specific regulation of E2F transactivation by cyclin/cdk2 complexes. *Genes Dev* 1994; **8**: 1772–1786.
63. Krek W, Ewen ME, Shirodkar S, Arany Z, Kaelin WG, Jr Livingston DM. Negative regulation of the growth-promoting transcription factor E2F1 by a stably bound cyclin A-dependent protein kinase. *Cell* 1994; **78**: 161–172.
64. Qin XQ, Livingston DM, Kaelin WG, Jr Adams PD. Deregulated transcription factor E2F1 expression leads to S-phase entry and p53-mediated apoptosis. *Proc Natl Acad Sci USA* 1994; **91**: 10918–10922.
65. Kowalik TF, DeGregori J, Scwartz JK, Nevins JR. E2F1 overexpression in quiescent fibroblasts leads to induction of cellular DNA synthesis and apoptosis. *J Virol* 1995; **69**: 2491–2500.
66. Fueyo J, Gornez-Manzano C, Yung WK, *et al*. Overexpression of E2F1 in glioma trigger apoptosis and suppresses tumor growth *in vitro* and *in vivo*. *Nat Med* 1998; **4**: 685–690.
67. Pomerantz J, Shreiber-Agus N, Liegeois N, *et al*. The ink4a tumor suppressor gene product, $p19^{ARF}$, interacts with MDM2 and neutralizes MDM2's inhibition of p53. *Cell* 1998; **92**: 713–723.
68. Zhang Y, Xiong Y, Yarbrourgh WG. ARF promotes MDM2 degradation and stabilizes p53: ARF-INK4a locus deletion impairs both the Rb and p53 tumor suppression pathways. *Cell* 1998; **92**: 725–734.
69. Hsieh J-K, Chan FSG, O'Connor DJ, Mittnacht S, Zhong S, Lu X. Rb regulates the stability and the apoptotic function of p53 via MDM2. *Mol Cell* 1999; **3**: 181–193.
70. Yap DB, Hsieh JK, Chan FS, Lu X. Mdm2: a bridge over the two tumor suppressors, p53 and Rb. *Oncogene* 1999; **18**: 7681–7689.
71. Loughran O, La Thangue NB. Apoptotic and growth-promoting activity of E2F modulated by MDM2. *Mol Cell Biol* 2000; **20**: 2186–2197.
72. Phillips AC, Bates S, Ryan KM, Helin K, Vousden KH. Induction of DNA synthesis and apoptosis are separable functions of E2F-1. *Genes Dev* 1997; **11**: 1853–1863.
73. Phillips AC, Ernst MK, Bates S, Rice NR, Vousden KH. E2F1 potentiates cell death by blocking anti-apoptotic signaling pathways. *Mol Cell* 1999; **4**: 771–781.
74. Stiewe T, Putzer BM. Role of p53-homologue p73 in E2F1-induced apoptosis. *Nat Genet* 2000; **26**: 464–469.
75. Pauvlovich AG, Toczyski DP, Hartwell LH. When checkpoints fail. *Cell* 1997; **88**: 315–321.
76. Lukas S, Sorensen CS, Kramer E, *et al*. Accumulation of cyclinB1 requires E2F and cyclin A-dependent rearrangement of the anaphase-promoting complex. *Nature* 1999; **401**: 815–818.
77. Morgenbesser SD, Williams BO, Jacks T, Depinho RA. P53 dependent apoptosis produced by Rb-deficiency in the developing mouse lens. *Nature* 1994; **371**: 72–74.
78. Symonds H, Krall L, Remington L, *et al*. p53-dependent apoptosis suppresses tumor growth and progression *in vivo*. *Cell* 1994; **78**: 703–711.
79. Pan H, Yin C, Dyson NJ, Harlow E, Yamasaki L, van Dyke T. Key roles for E2F1 in p53-dependent apoptosis and in cell division within developing tumors. *Mol Cell* 1998; **2**: 283–292.

